Applied Energy 381 (2025) 125045

Contents lists available at ScienceDirect

Applied Energy

journal homepage: www.elsevier.com/locate/apenergy

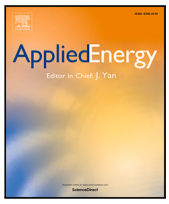

Enhancing power system reliability through demand flexibility of Grid-Interactive Efficient Buildings: A thermal model-based optimization approach

Miloš Pantoš *, Lucija Lukas

University of Ljubljana, Faculty of Electrical Engineering, Slovenia

ARTICLE INFO

Keywords:
Expected energy not supplied
Linear programming
Loss of load expectation
Optimization
Power system reliability
Thermal model of a building

ABSTRACT

The paper evaluates the impact of grid-interactive efficient buildings (GEBs) on power system reliability. To achieve this, a single-zone thermal model of a building is developed, allowing for the simulation of indoor temperature dynamics based on the characteristics of the building envelope and internal thermal mass. The potential of GEBs to adjust their electric consumption, recognized as demand flexibility, is integrated into the direct optimization of reliability indices, specifically Loss of Load Expectation (LOLE) and Expected Energy Not Supplied (EENS). The analysis is conducted using the proposed optimization model in two distinct case studies. In the first scenario, households do not support the power system and only optimize their energy consumption for heating and cooling. In the second scenario, households provide available demand flexibility of GEBs to the power system to enhance reliability. This demand flexibility is constrained by the need to maintain indoor temperature within limits that ensure comfortable use of the space. The analysis highlights the potential of GEBs to improve power system reliability by reducing LOLE and EENS. The primary scientific contribution of this research is the development of an optimization model that incorporates a thermal model of GEBs without assuming a generic demand flexibility for the buildings.

1. Introduction

As buildings consume a significant portion of electricity, namely the electrification rate in the building sector reached 47.19% in 2020, [1], their role in power system operations is becoming more critical, particularly in managing the uncertainties introduced by intermittent renewable energy sources and load flexibility. By utilizing variable resources and demand, buildings can stabilize their interactions with the power system and participate in demand response (DR) programs, helping to balance supply and demand, [2,3]. GEBs, characterized by their flexibility, stability, and independence, are designed to optimize energy use, manage loads effectively, and support grid reliability, [4]. These buildings not only reduce the burden on the system by minimizing interaction volatility but also actively contribute to system stability by adjusting their operations in response to system needs, particularly during peak demand periods or supply shortages, [4].

1.1. Motivation

Historically, power system planning relied on deterministic approaches with "N-1" contingency analyses. However, with the rise of uncertainties in renewable energy production and the reliability of controllable and communication devices, stochastic approaches are becoming increasingly important. Moreover, societal awareness of sustainable and environmentally acceptable infrastructure development is pressuring network planners to maximize the potential of existing power systems, rather than simply investing in new equipment.

In this perspective, GEBs will play in the future a pivotal role in the shift from conventional methods to advanced approaches for power system planning. This transformation introduces the potential of new technologies such as demand flexibility of GEBs through energy storage systems, hydrogen technologies, electric-drive vehicles, controllable devices and renewable energy sources with intermittent production. In this context, GEBs offer a critical advantage by integrating smart controls that optimize energy consumption and provide grid services, thus enhancing system resilience and reliability, [5,6]. In general, GEBs support the broader energy system by integrating distributed energy resources and facilitating the transition to net-zero emissions, [7]. As active participants in the energy ecosystem, GEBs are essential for a sustainable and resilient energy future, [5,6].

* Corresponding author.
E-mail addresses: milos.pantos@fe.uni-lj.si (M. Pantoš), lucija.lukas@fe.uni-lj.si (L. Lukas).

https://doi.org/10.1016/j.apenergy.2024.125045
Received 4 September 2024; Received in revised form 18 November 2024; Accepted 27 November 2024
Available online 16 December 2024

Nomenclature

Abbreviations

COP	Coefficient of performance.
CS	Case study.
DR	Demand response.
EENS	Expected Energy Not Supplied.
GEB	Grid-interactive efficient buildings.
HVAC	Heating, ventilation, and air conditioning.
LOLE	Loss of Load Expectation.
MILP	Mixed-integer linear program.
PV	Photovoltaic.
RC	Resistances and Capacitances.

Sets and indices

$i \in \mathcal{I}$	Set of possible resource capacity states i.
$j \in \mathcal{J}$	Set of elements in the building envelope j.
$t \in \mathcal{T}$	Set of time slots t.
Ω	Set of optimization variables.
0	Index for initial state.

Variables

$\alpha \in \{0,1\}$	Indicator variable.
$x \in \mathbb{R}$	Demand flexibility in positive direction.
$b \in \mathbb{R}$	Demand flexibility in negative direction.
$T \in \mathbb{R}$	Temperature.
$Q \in \mathbb{R}$	Thermal energy (hear, cool).
$\beta \in \{0,1\}$	Indicator variable.

Matrices

T	State vector.
A	System matrix.
B	Input matrix.
U	Input vector.

Subscripts (descriptors)

o	Outside.
i	Inside.
w	Wall.
win	Window.
sol	Solar.
z	Zone, zonal.

Superscripts (descriptors)

indoor	Indor.
heat	Heating.
cool	Cooling.
min	Minimum.
max	Maximum.
PS	Power system.
H	Household.
CS	Case study.

Constants and parameters

S	Number of time slots t.
p	Probability of state.
d	Duration of unsufficient generation capacity.
w	Curtailed energy due to the capacity outage.
a	Number of generators.
A	Availability of generator.
U	Unavailability of generator.
R	Thermal resistance.
C	Thermal capacitance.
Q	Thermal energy (indoor, sol, win).
P	Power.
COP	Coefficient of performance.
M	Large positive number.

Example

$T_{z,t}^{\max}$	Maximum zone temperature in time slot t.

1.2. Related work

Numerous applications of GEBs in power system operation are proposed by different researchers. For example, the article [8], proposes a hierarchical model-based scheme to enhance the operation of power systems by aggregating and activating the energy flexibility of multi-zone buildings. It introduces a novel approach where an aggregator manages energy consumption across building zones, ensuring that buildings remain committed to their energy bids in the power market while maintaining comfort levels. The method improves power system operation by optimizing energy use and providing real-time regulation capabilities.

A coordinated voltage regulation strategy that integrates buildings with the distribution network by leveraging the flexibility of distributed energy resources, including the heating, ventilation, and air conditioning (HVAC) systems, is presented in [9]. The proposed method utilizes model predictive control to optimize power flow and reactive power control, enabling buildings to actively participate in voltage control. This approach enhances the stability and efficiency of the distribution network while simultaneously optimizing building energy management, ensuring that both voltage levels and energy usage are maintained within desired limits.

The article [10] explores demand-side flexibility and demand-side bidding strategies for managing flexible loads in air-conditioned buildings. It focuses on how buildings can optimize their participation in electricity markets by adjusting HVAC system operations to bid for and utilize demand-side flexibility. The study provides insights into building energy modelling and management, with a particular emphasis on applications in Singapore's power system, contributing to more efficient energy use and enhanced grid stability through demand-side management practices.

The study [11] proposes a novel distributed sliding mode control approach for aggregating the demand response of grid-interactive smart buildings to support power system frequency regulation, enhancing the stability and efficiency of the grid through decentralized coordination.

A strategy for integrated energy collaborative optimal dispatch within smart grids, incorporating energy-flexible buildings, is presented in [12]. The proposed solution introduces a model that integrates energy DR with thermal resistance modelling of buildings to enhance load management and grid stability. This approach allows for more efficient dispatch of energy resources by leveraging the flexibility of building energy consumption, contributing to the overall optimization of smart grid operations.

The research presented in [13] investigates the cost-optimal operation of a flexible building equipped with local photovoltaic (PV) systems in a Singaporean environment. It presents an optimization model that balances energy consumption, PV generation, and grid interaction to minimize costs while considering demand response strategies.

The study contributes to smart grid operations by demonstrating how flexible buildings can effectively integrate renewable energy sources, optimize energy use, and reduce reliance on the grid through efficient scheduling and forecasting methods.

A critical aspect of research on GEBs and buildings in general is the development of a thermal model that accurately incorporates the thermal properties of the building envelope and internal thermal mass. This ensures a comprehensive representation of the building's energy dynamics.

The existing literature provides several different thermal models of buildings that range from simple empirical models to highly detailed physical models. The choice of model depends on the desired accuracy, complexity, data availability and computational resources available. Among the various approaches, grey-box models and resistances and capacitances (RC) models are particularly popular due to their balance between accuracy and computational efficiency, [14].

Grey-box models, [15], combine the physical insights of white-box models, [15], which are based on detailed physical principles, with the simplicity and flexibility of black-box models, [15], which are purely data-driven. Grey-box models typically incorporate a simplified representation of the building's physical characteristics while using measured data to calibrate the model parameters. This approach allows for the inclusion of key thermal dynamics, such as heat transfer through the building envelope and the thermal inertia of the structure, without requiring the detailed specifications necessary for white-box models. Grey-box models are commonly used for control-oriented applications, such as model predictive control of HVAC systems, where a detailed understanding of the building's thermal response is necessary, but the model needs to be computationally efficient. These models are also employed in demand response strategies, where buildings adjust their energy consumption in response to external signals from the grid. A typical grey-box model of a building might represent the building's thermal behaviour using a small number of lumped thermal capacitances and resistances, which approximate the heat storage and transfer characteristics of the building. The parameters of these elements are often estimated using system identification techniques, based on measured temperature and energy use data, [16].

RC models are a specific type of grey-box model that represent the thermal behaviour of a building using electrical analogies, i.e. resistors (R) for thermal resistances and capacitors (C) for thermal capacitances. In an RC model, the building is conceptualized as a network of resistors and capacitors. Thermal resistances represent the resistance to heat flow (e.g., through walls, windows), and thermal capacitances represent the ability of the building's mass to store heat. The interactions between these elements describe the dynamic thermal behaviour of the building. RC models can vary in complexity. Simple RC models might use a single resistor and capacitor to represent the entire building, focusing on the overall heat balance. More complex RC models might include multiple resistors and capacitors to represent different building components (e.g., walls, windows, internal mass) and their interactions.

The simplest form is the 1R1C model, with one resistor representing the overall thermal resistance and one capacitor representing the overall thermal capacitance. The 2R1C model includes two resistors representing the heat transfer through the building envelope and internal mass and one capacitor, and the 3R2C model is more detailed model since it adds an extra layer of complexity by separating the building envelope and internal thermal mass into distinct thermal paths. There have been many improvements in the RC model over the years such as the 3R4C and 4R5C models that enable even more accurate modelling required for some detailed analysis of thermal dynamics of buildings. A critical review of grey-box modelling is provided in [17].

RC models are relatively easy to develop and computationally efficient, making them suitable for real-time applications like predictive control. However, their accuracy depends heavily on the correct identification of parameters, and they may not capture all the nuances of a building's thermal behaviour, especially in buildings with complex geometries or varying thermal properties. RC models are widely used in building energy management systems for tasks such as energy forecasting, demand-side management, and optimizing HVAC operations. Due to their simplicity, they are particularly useful in applications where computational resources are limited or where fast simulation times are required.

1.3. Knowledge gap

The primary knowledge gap in the existing literature centres on how to effectively model the contribution of household flexible demand in GEBs to power system reliability. While significant attention has been given to power system operation, the integration of power system planning, particularly in assessing reliability metrics such as LOLE and EENS, remains underexplored. Although thermal models of buildings exist, there is a critical need to develop models that not only incorporate these thermal dynamics but also integrate power system reliability indices like LOLE and EENS. This integration is essential for a more comprehensive analysis of how GEBs can support both the operational and planning aspects of power systems, ultimately enhancing overall system reliability.

1.4. Contributions

This paper builds on our previous work [18] by advancing the optimization model for power system reliability, with a particular focus on metrics such as LOLE and EENS, through the integration of GEBs into the power system planning process. To achieve this, we develop an advanced optimization model that maximizes power system reliability by incorporating the thermal characteristics of buildings alongside traditional reliability measures. This integrated approach offers a more holistic framework for assessing and improving the reliability of power systems by leveraging the flexibility potential of GEBs.

In this research, the 3R2C model is employed due to its widespread use in modelling transient heat transfer in building envelopes. This model accurately represents the behaviour of indoor temperature in response to various thermal inputs, including space heating, cooling, solar radiation (walls and windows), and occupant activities. Additionally, it accounts for the thermal properties of the building envelope and internal thermal mass, ensuring a comprehensive representation of the building's energy dynamics.

The objective of this research is to harness the inherent flexibility of HVAC systems in GEBs within the power system planning process. By doing so, the aim is to enhance power system reliability in a more sustainable manner, reducing the need for additional investments in power infrastructure, including new generation sources, transmission capacities, energy storage systems, and other technologies, while also supporting the reliable operation of the power system.

The findings are particularly valuable for transmission and distribution system operators involved in system planning, as well as for building owners who contribute to ancillary services that enhance system reliability.

1.5. Novelty of the proposed approach

The novelty of the proposed solution lies in integrating the 3R2C thermal model for GEBs into the optimization of reliability indices, specifically LOLE and EENS, as presented in [18]. This approach represents a significant advancement by extending traditional reliability optimization methods to account for the dynamic thermal behaviour of GEBs. Unlike traditional models, which often generalize building demand flexibility without considering specific temperature control dynamics, our model incorporates these dynamics to capture temperature-driven demand flexibility in real-time scenarios. By utilizing a single-zone thermal model, this study provides a foundational analysis of GEB impacts on LOLE and EENS, allowing for precise evaluations of

their role in grid stability and resilience. This single-zone model enables computational feasibility while laying the groundwork for future extensions to more complex scenarios, such as multi-zone or multi-building frameworks with diverse thermal characteristics and demand flexibility.

The choice of a single-zone thermal model enables a focused analysis of the interactions between indoor temperature control and power system reliability. This model provides a computationally feasible framework to evaluate the effects of temperature-based demand flexibility on reliability metrics like LOLE and EENS. Although it is a simplified representation, the single-zone model captures key dynamics necessary for understanding GEB contributions to grid stability. This choice serves as a foundational approach, allowing for extensions to multi-zone and multi-building scenarios in future work.

1.6. Organization of the paper

The remainder of this paper is organized as follows: Section 2 presents the reliability indices LOLE and EENS that are later applied in the proposed power system reliability optimization, Section 3 introduces the thermal model of GEBs that is incorporated in the proposed optimization model for power system reliability support provided by GEBs presented in Section 4; results are analysed and discussed in detail in Section 5, followed by the final Section 6, which concludes the paper and provides directions for future work.

2. Power system reliability

This research focuses on maximizing power system reliability through the demand response of HVAC systems installed in households. The objective is to demonstrate the impact of controlled HVAC operations as an ancillary service on power system reliability, measured by the well-known and widely used indices, Loss of Load Expectation (LOLE) and Expected Energy Not Supplied (EENS). Specifically, these indices serve as measures of resource adequacy, which is a critical component of system reliability.

2.1. Reliability indices

LOLE represents the expected number of hours during which the available generation capacity is insufficient to meet demand. It is calculated using the following equation:

$$LOLE = \sum_{i \in I} p_i d_i, \tag{1}$$

where p_i represents the probability of state i with a particular generation configuration, d_i is obtained from the load duration curve and represents the duration during which load demand exceeds the remaining capacity P_i, and I is the set of possible generation states. For multiple generators, the calculation considers all possible states, making LOLE a demanding yet essential reliability metric. If a generators are considered, 2^a capacity states are possible since each generator can either operate as scheduled with a probability defined by its availability A, represented by status '1', or be out of operation with a probability defined by its unavailability $U = 1 - A$, represented by status '0'. Therefore, in the case of numerous generators, calculating the reliability indices LOLE and EENS becomes computationally demanding, as all combinations of operating statuses of generators ('in operation - 1' and 'out of operation - 0') must be considered. Fig. 1 presents the load duration curve with defined d_i.

The EENS index calculates the total energy not supplied due to capacity shortages:

$$EENS = \sum_{i \in I} p_i w_i, \tag{2}$$

where w_i represents the curtailed energy due to outages in state i, as illustrated in Fig. 1. These indices are foundational to power system reliability assessments and serve as direct outputs of the proposed optimization model.

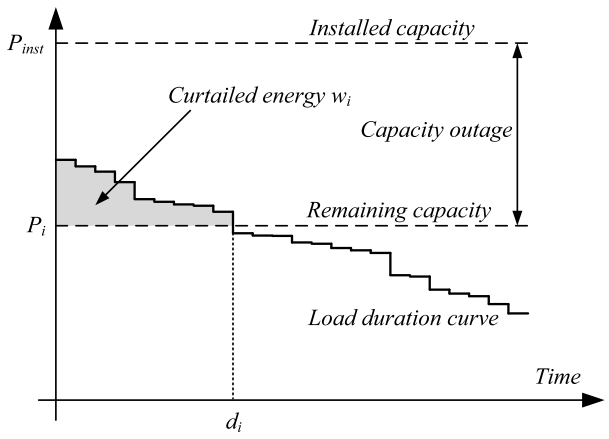

Fig. 1. Load duration curve with d_i and w_i.

2.2. Role of load forecasting in demand flexibility

Accurate load forecasting is crucial for the demand flexibility of GEBs, as it enables the model to anticipate and adapt to various load types that affect grid reliability. Load forecasting enhances the model's ability to optimize demand-side flexibility, allowing GEBs to adjust their consumption patterns in response to system demands effectively. This approach aligns with recent advancements in load forecasting, which improve demand response strategies through better predictive accuracy.

Prior studies have demonstrated effective methods for forecasting complex, dynamic load profiles. For instance, [19,20] have laid foundational work in capturing varied load characteristics, enabling more reliable and responsive demand-side management. These studies inform the load forecasting techniques integrated into our model, ensuring a robust basis for evaluating GEB impacts on LOLE and EENS.

2.3. Integrating thermal model and reliability metrics

After defining the reliability indices, a thermal model of the building must be introduced to accurately model the limits of the building's demand response capacity, which is incorporated into the maximization of power system reliability. The primary goal is to maintain the indoor temperature within predefined limits that ensure comfortable use of the space. The building envelope and its characteristics, internal thermal mass, and space properties, as well as internal thermal sources including the HVAC system, have the most significant impact on temperature. The building possesses a certain thermal inertia, which allows for adjustments in electricity consumption for heating and cooling without causing discomfort to the occupants due to overheating or excessive cooling. This flexibility enables the electric power system to be reliably supported.

To support demand flexibility, we utilize the 3R2C thermal model, which provides an accurate yet computationally feasible representation of building thermal dynamics. This model captures key factors like indoor heating and cooling, solar radiation, and occupancy. The thermal response of GEBs, modelled within a single-zone setup, allows for precise adjustments in HVAC operations, maintaining indoor temperatures within comfort thresholds while contributing to power system reliability. This thermal modelling forms part of our optimization process, where load forecasting informs adjustments to HVAC setpoints, aligning GEB flexibility with grid reliability needs.

The final optimization model integrates load forecasting, thermal dynamics, and reliability indices to minimize LOLE and EENS. By leveraging mixed-integer linear programming, we dynamically control HVAC operations in response to real-time load forecasts. This approach

enables GEBs to act as active participants in grid stability, offering a sustainable solution that aligns with resource adequacy requirements.

The thermal model employed in this study was calibrated using standard building energy profiles, which are widely accepted in grid-interactive efficient building research. To ensure the validity and reliability of the experimental setup, the measured data used in this study were derived from these standard profiles, which represent realistic scenarios for residential energy consumption. These profiles were calibrated and validated against existing methodologies in the literature to align with established frameworks. While direct comparisons with real-world data were not part of this study, future work will incorporate real-world validation to further strengthen the reliability of the proposed model. These profiles provide realistic data for indoor temperature dynamics and energy consumption, ensuring the model's consistency with existing frameworks. While the model's performance aligns with established methodologies, direct validation with real-world data was beyond the scope of this study. However, this validation is planned for future research to further ensure its applicability and reliability under diverse conditions.

3. Thermal model of a building

The RC (Resistance-Capacitance) thermal network model is a widely used approach for representing the thermal dynamics of buildings. This model effectively captures the thermal delays caused by the building envelope and internal thermal mass, providing robust and accurate estimates of the heating and cooling loads alongside indoor temperature variations. The RC model leverages the principle of analogy between two different physical domains, thermal and electrical, that can be described by analogous mathematical equations. Specifically, the building is represented as a linear electrical circuit, with the resulting state-space equations derived from solving that circuit. In this analogy, temperature corresponds to voltage, heat flux to current, thermal resistance to electrical resistance, and thermal capacitance to electrical capacitance. The equivalent circuit of the building is then constructed by assembling the models of individual components such as walls, windows, and internal mass.

Over the years, the RC model has seen various improvements, such as the development of the 3R4C and 4R5C models. However, in this research, the 3R2C model is utilized due to its balance between accuracy and computational efficiency.

In the 3R2C model, the building envelope, comprising walls, roof, and floor, is represented by an RC circuit, as shown in Fig. 2. Here, T_{o} represents the ambient temperature, $T_{\mathrm{wo},j}$ is the temperature on the outside surface of wall j, $T_{\mathrm{wi},j}$ is the temperature on the internal surface of wall j, and T_{z} denotes the zone temperature within the building. The parameters $R_{\mathrm{o},j}$ and $R_{\mathrm{i},j}$ represent the thermal convective resistances of the ambient air and the zone air, respectively. $R_{\mathrm{w},j}$ represents the thermal conductive resistance of wall j, while $C_{\mathrm{w},j}$ denotes the thermal capacitance of the wall.

For this research, a single-zone model is employed to describe the building. Interior walls are considered part of the internal thermal mass, while exterior walls form the building envelope. To simplify the model, the following assumptions are introduced:

- The building envelope is modelled as an ideal rectangle, consisting of four walls, a floor, and a flat roof. The roof is treated as a vertical wall and is modelled using the same network structure as the walls.
- The zone air is assumed to be ideally mixed, resulting in a uniform internal temperature.
- Each wall contains a window, which does not accumulate thermal energy and is therefore represented by a simple thermal resistance.

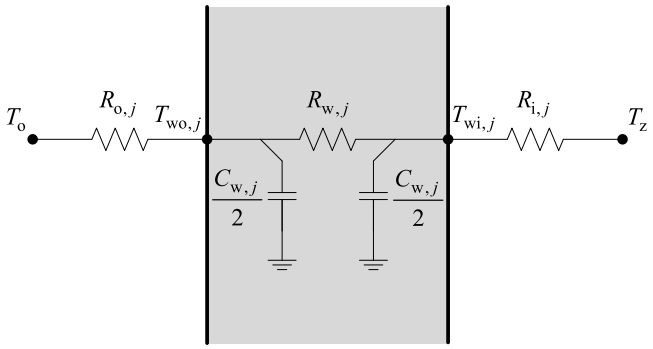

Fig. 2. Structure of the 3R2C model of the building envelope j.

- The RC parameters are assumed to be time-invariant.
- The active elements in the building's thermal circuit include outdoor air temperature, solar radiation on the walls, roof and windows, and internal thermal sources.
- Internal heat flux arises from internal thermal sources, such as the activities of building occupants and the operation of electrical appliances, including HVAC systems.
- The floor surface is considered adiabatic.

Fig. 3 illustrates the 3R2C thermal network model applied in this research. The roles of the RC parameters in relation to the walls and roof are as explained in Fig. 2. Additionally, windows are modelled as thermal resistances $R_{\mathrm{win},j}$ with solar radiations entering the space $Q_{\mathrm{win,sol},j}$, where j corresponds to each of the four walls. The symbol Q_{z} represents the total internal thermal sources, which include indoor activities of the building occupants, denoted as $Q_{\mathrm{z}}^{\mathrm{indoor}}$, and electrical appliances including heating and cooling provided by the HVAC system, denoted as $Q_{\mathrm{z}}^{\mathrm{heat}}$ and $Q_{\mathrm{z}}^{\mathrm{cool}}$, respectively:

$$Q_{\mathrm{z}} = Q_{\mathrm{z}}^{\mathrm{indoor}} + Q_{\mathrm{z}}^{\mathrm{heat}} - Q_{\mathrm{z}}^{\mathrm{cool}}. \tag{3}$$

The symbol C_{z} in Fig. 3 denotes the thermal capacitance of the zone air.

The main output of the model is the indoor temperature T_{z}, which is influenced by several inputs: outdoor air temperature T_{o}, solar radiations $Q_{\mathrm{sol},j}$ and $Q_{\mathrm{win,sol},j}$, and internal sources Q_{z}. The temperatures $T_{\mathrm{ow},j}$ and $T_{\mathrm{oi},j}$ are also outputs of the model, although they are not the primary focus of this research.

To further simplify the network model shown in Fig. 3, an equivalent network model, as depicted in Fig. 4, is introduced. The equivalent RC parameters and solar radiations are calculated as follows:

$$R_{\mathrm{o}} = \left(\sum_{j \in \mathcal{J}} \frac{1}{R_{\mathrm{o},j}} \right)^{-1}, \tag{4}$$

$$R_{\mathrm{w}} = \left(\sum_{j \in \mathcal{J}} \frac{1}{R_{\mathrm{w},j}} \right)^{-1}, \tag{5}$$

$$R_{\mathrm{i}} = \left(\sum_{j \in \mathcal{J}} \frac{1}{R_{\mathrm{i},j}} \right)^{-1}, \tag{6}$$

$$R_{\mathrm{win}} = \left(\sum_{j \in \mathcal{J}} \frac{1}{R_{\mathrm{win},j}} \right)^{-1}, \tag{7}$$

$$C_{\mathrm{w}} = \sum_{j \in \mathcal{J}} C_{\mathrm{w},j}, \tag{8}$$

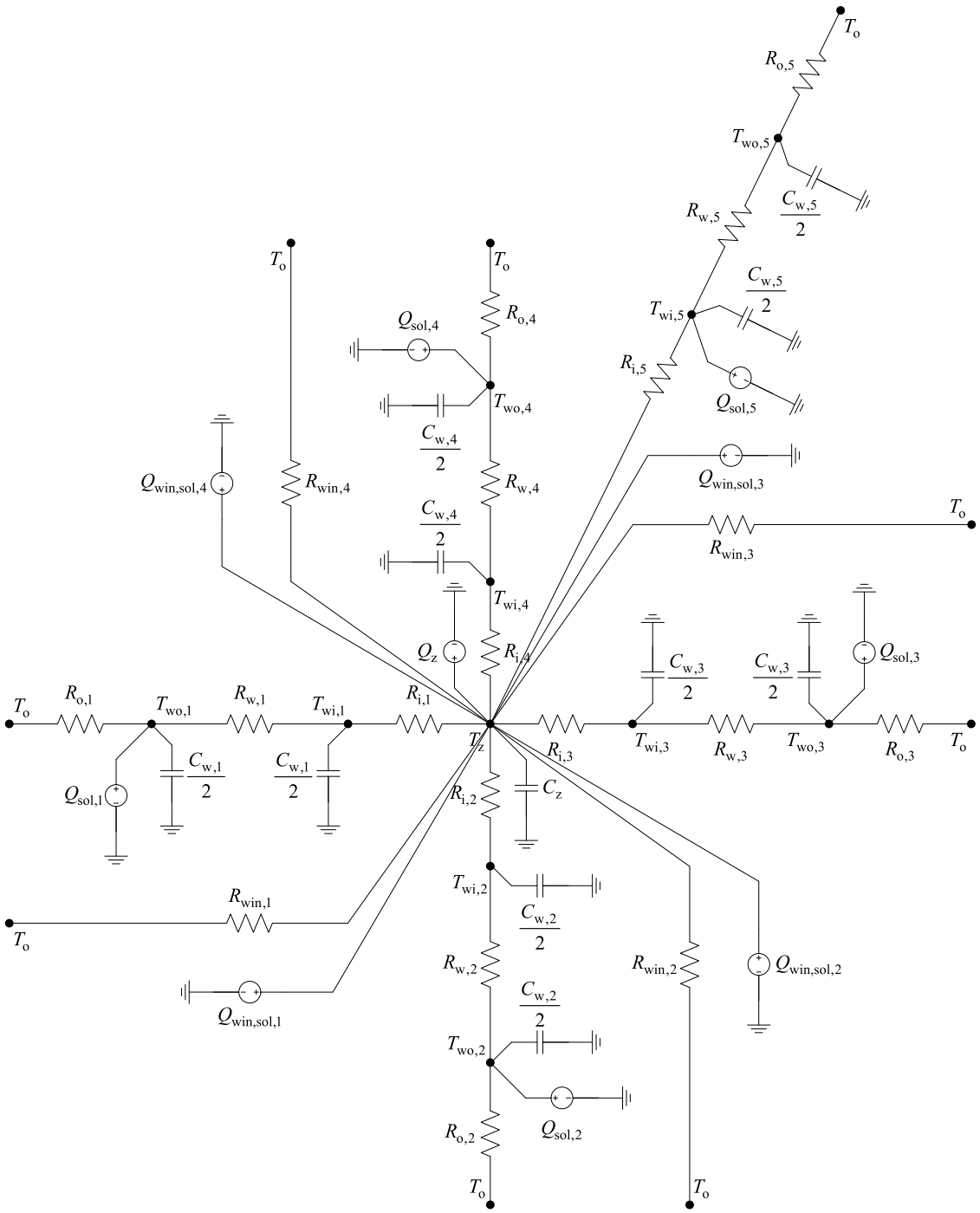

Fig. 3. The 3R2C thermal network model.

$$Q_{\text{sol}} = \sum_{j \in \mathcal{J}} Q_{\text{sol},j}, \tag{9}$$

$$Q_{\text{win,sol}} = \sum_{j \in \mathcal{J}} Q_{\text{win,sol},j}, \tag{10}$$

where $\mathcal{J}$ represents the set of five elements that constitute the building envelope, i.e., the four walls and the roof.

The equivalent network model shown in Fig. 4 can be represented in state-space form by a set of first-order differential equations:

$$\begin{aligned} \frac{\mathrm{d}T_{\text{wo}}}{\mathrm{d}t} = &- \frac{2}{C_{\text{w}}}\left(\frac{1}{R_{\text{o}}} + \frac{1}{R_{\text{w}}}\right) T_{\text{wo}} + \frac{2}{C_{\text{w}}}\left(\frac{1}{R_{\text{o}}} T_{\text{o}} + \frac{1}{R_{\text{w}}} T_{\text{wi}}\right) \\ &+ \frac{2}{C_{\text{w}}} \dot{Q}_{\text{sol}}, \end{aligned} \tag{11}$$

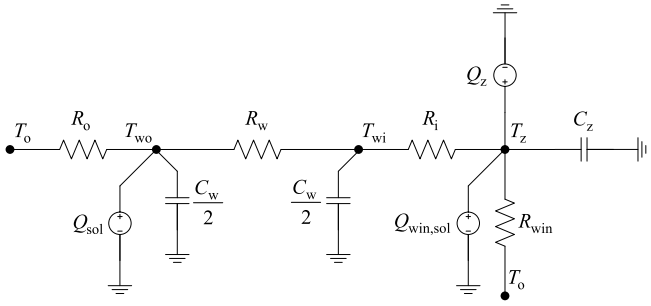

Fig. 4. Equivalent of the 3R2C thermal model.

$$\frac{dT_{wi}}{dt} = -\frac{2}{C_w}\left(\frac{1}{R_w}+\frac{1}{R_i}\right)T_{wi} + \frac{2}{C_w}\left(\frac{1}{R_w}T_{wo}+\frac{1}{R_i}T_z\right), \tag{12}$$

$$\frac{dT_z}{dt} = -\frac{1}{C_z}\left(\frac{1}{R_{win}}+\frac{1}{R_i}\right)T_z + \frac{1}{C_z}\left(\frac{1}{R_{win}}T_o+\frac{1}{R_i}T_{wi}\right) + \frac{1}{C_z}\left(\dot{Q}_z^{indoor}+\dot{Q}_z^{heat}-\dot{Q}_z^{cool}+\dot{Q}_{win,sol}\right). \tag{13}$$

It is important to note that the state-space representation of the thermal dynamics of the building depends solely on the temperatures T_{wo}, T_{wi}, and T_z. From Eqs. (11)–(13), it can be seen that the indoor temperature T_z is influenced by the outdoor temperature T_o, solar radiations Q_{sol} and $Q_{win,sol}$, and internal heat flux Q_z. By defining the state vector **T** and input vector **U** as follows:

$$\mathbf{T} = \begin{bmatrix} T_{wo} \\ T_{wi} \\ T_z \end{bmatrix}, \tag{14}$$

$$\mathbf{U} = \begin{bmatrix} T_o \\ \dot{Q}_z^{indoor} \\ \dot{Q}_z^{heat} \\ \dot{Q}_z^{cool} \\ \dot{Q}_{win,sol} \\ \dot{Q}_{sol} \end{bmatrix}, \tag{15}$$

the state-space model is expressed as

$$\dot{\mathbf{T}} = \mathbf{A}\cdot\mathbf{T} + \mathbf{B}\cdot\mathbf{U}, \tag{16}$$

where matrices **A** and **B** are given by

$$\mathbf{A} = \begin{bmatrix} -\frac{2}{C_w}\left(\frac{1}{R_o}+\frac{1}{R_w}\right) & \frac{2}{C_w R_w} & 0 \\ \frac{2}{C_w R_w} & -\frac{2}{C_w}\left(\frac{1}{R_w}+\frac{1}{R_i}\right) & \frac{2}{C_w R_i} \\ 0 & \frac{1}{C_z R_i} & -\frac{1}{C_z}\left(\frac{1}{R_{win}}+\frac{1}{R_i}\right) \end{bmatrix}, \tag{17}$$

$$\mathbf{B} = \begin{bmatrix} \frac{2}{C_w R_o} & 0 & 0 & 0 & 0 & \frac{2}{C_w} \\ 0 & 1 & 1 & 1 & 1 & 0 \\ \frac{1}{C_z R_{win}} & \frac{1}{C_z} & \frac{1}{C_z} & -\frac{1}{C_z} & \frac{1}{C_z} & 0 \end{bmatrix}. \tag{18}$$

The state-space model described in Eqs. (14)–(18) forms the basis for simulating the thermal behaviour of the building under different conditions, which is crucial for predicting the HVAC system's performance and optimizing energy consumption while maintaining comfort. This model will be used to simulate different energy management strategies and determine their effectiveness in maintaining the desired indoor conditions with minimal energy use.

4. Optimization of power system reliability with grid-interactive efficient buildings

To maximize power system reliability, the selected indices, Loss of Load Expectation (LOLE) and Expected Energy Not Supplied (EENS), must be minimized. This optimization problem is formulated as a mixed-integer linear program (MILP) with the objective function:

$$J = \underset{\Omega}{\text{minimize}} \sum_{i\in I}\sum_{t\in T}\left(p_i\alpha_{i,t}\right), \tag{19}$$

where $\alpha_{i,t}$ is an indicator variable for state i and time slot t, defined as:

$$\alpha_{i,t} = \begin{cases} 1 & \text{for} \quad P_i - \left(P_t + x_t - b_t\right) < 0 \\ 0 & \text{for} \quad P_i - \left(P_t + x_t - b_t\right) \geq 0 \end{cases}. \tag{20}$$

This indicator variable is binary, taking values of 0 or 1 based on the condition in Eq. (20). Fig. 5 graphically illustrates this condition for states i and $i+1$. Here, P_t represents the electric power consumption during time slot t as part of the initial load profile, while P_i represents the remaining capacity in state i. The load duration curve shown in Fig. 1 is derived from the electric power consumption P_t, as illustrated by the bold line in Fig. 5. The variables x_t and b_t are continuous optimization variables that adjust demand flexibility in both positive and negative directions. Consequently, $P_t + x_t - b_t$ in Eq. (20) and Fig. 5 represents the optimal load profile in time slot t, maximizing system reliability.

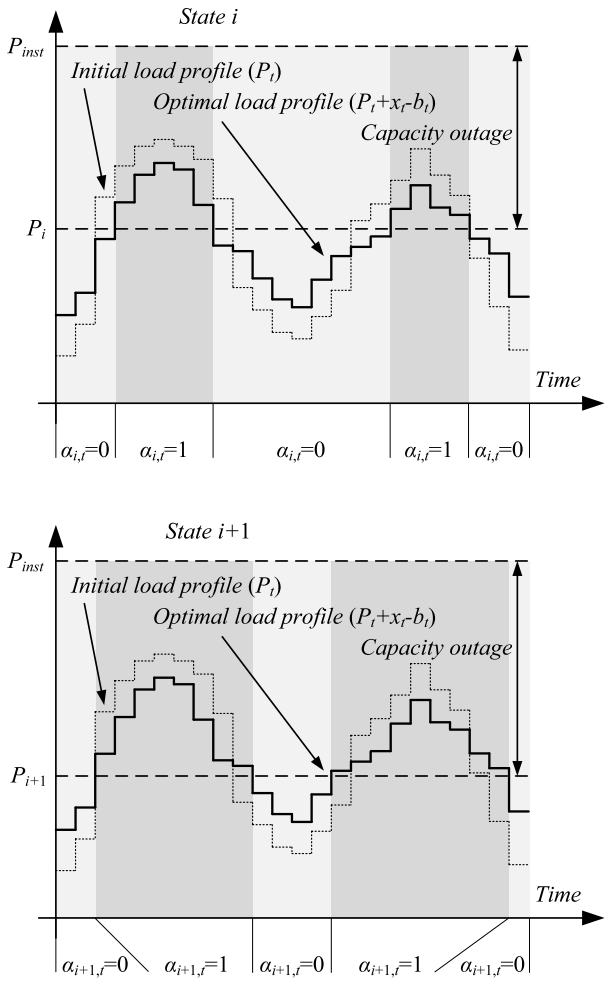

Fig. 5. Indicator variable $\alpha_{i,t}$.

Demand flexibility can be achieved using various technologies, such as energy storage systems or electric vehicles, where x_t and b_t represent the charged and discharged energy in time slot t, respectively. This approach is discussed in [18].

In this study, x_t and b_t represent changes in electric power consumption P_t during time slot t due to the operation of HVAC systems in households. Specifically, heating, ventilation, and cooling account for additional electric energy consumption required to maintain the indoor temperature $T_{z,t}$ within acceptable limits. This consumption is optimally distributed over the observation period to maximize system reliability.

In Section 3, the building's thermal model is presented without considering time dependency. However, the active elements of the building's thermal circuit (outdoor air temperature, solar radiation on walls, roof and windows, internal thermal sources) and the indoor temperature T_z are time-dependent. Thus, the correct notation is $T_{z,t}$ to reflect this time dependency.

The objective function in Eq. (19) is subject to the following constraint:

$$\dot{\mathbf{T}}_t = \mathbf{A}\cdot\mathbf{T}_t + \mathbf{B}\cdot\mathbf{U}_t, \tag{21}$$

where $\mathbf{T}_t$ and $\mathbf{U}_t$ are time-dependent matrices with time-dependent elements:

$$\mathbf{T}_t = \begin{bmatrix} T_{\mathrm{wo},t} \\ T_{\mathrm{wi},t} \\ T_{\mathrm{z},t} \end{bmatrix}, \tag{22}$$

$$\mathbf{U}_t = \begin{bmatrix} T_{\mathrm{o},t} \\ \dot{Q}^{\mathrm{indoor}}_{\mathrm{z},t} \\ \dot{Q}^{\mathrm{heat}}_{\mathrm{z},t} \\ \dot{Q}^{\mathrm{cool}}_{\mathrm{z},t} \\ \dot{Q}_{\mathrm{win,sol},t} \\ \dot{Q}_{\mathrm{sol},t} \end{bmatrix}. \tag{23}$$

The matrices $\mathbf{A}$ and $\mathbf{B}$ contain the time-invariant RC parameters, as noted previously.

Eq. (21) can be expanded as:

$$\mathbf{T}_1 = \mathbf{T}_0 + \mathbf{A} \cdot \mathbf{T}_0 + \mathbf{B} \cdot \mathbf{U}_0, \tag{24}$$

$$\mathbf{T}_t = \mathbf{T}_{t-1} + \mathbf{A} \cdot \mathbf{T}_{t-1} + \mathbf{B} \cdot \mathbf{U}_{t-1} \quad \forall t = 2, \ldots, T, \tag{25}$$

where $\mathbf{T}_0$ and $\mathbf{U}_0$ represent initial state optimization variables $T_{\mathrm{wo},0}$, $T_{\mathrm{wi},0}$, $T_{\mathrm{z},0}$ and inputs $T_{\mathrm{o},0}$, $\dot{Q}^{\mathrm{indoor}}_{\mathrm{z},0}$, $\dot{Q}^{\mathrm{heat}}_{\mathrm{z},0}$, $\dot{Q}^{\mathrm{cool}}_{\mathrm{z},0}$, $\dot{Q}_{\mathrm{win,sol},0}$, $\dot{Q}_{\mathrm{sol},0}$. The symbol S denotes the number of time slots t in the observed period $\mathcal{T}$.

The optimization objective in Eq. (19) is also constrained by the indoor temperature, which must remain within predefined limits $T^{\min}_{\mathrm{z},t}$ and $T^{\max}_{\mathrm{z},t}$ to ensure occupant comfort. These comfort limits for indoor temperature are typically defined based on commonly accepted standards for thermal comfort in residential buildings. In the optimization model, these limits are enforced through explicit inequality constraints, ensuring that the indoor temperature remains within the specified range throughout the simulation:

$$T^{\min}_{\mathrm{z},t} \leq T_{\mathrm{z},t} \leq T^{\max}_{\mathrm{z},t}. \tag{26}$$

The final constraint describes the relationship between the heating and cooling needs of a building, $Q^{\mathrm{heat}}_{\mathrm{z},t}$ and $Q^{\mathrm{cool}}_{\mathrm{z},t}$, and the additional electricity consumption required to meet those needs. To properly account for the efficiency of the heating and cooling systems, the coefficient of performance (COP) must be considered. For heating, the COP represents the ratio of heat output to the electrical input, while for cooling, it represents the ratio of heat removed to the electrical input. The relationship can be expressed as:

$$x_t = \frac{\dot{Q}^{\mathrm{heat}}_{\mathrm{z},t}}{COP_{\mathrm{heat}}} + \frac{\dot{Q}^{\mathrm{cool}}_{\mathrm{z},t}}{COP_{\mathrm{cool}}}, \tag{27}$$

where COP_{heat} and COP_{cool} are the coefficients of performance for heating and cooling, respectively. The total electricity consumption x_t is constrained by a minimum value $x_{\min}$, typically set to 0, and a maximum value $x_{\max}$, which corresponds to the installed power capacity of the HVAC system. This ensures that the system operates within its feasible limits:

$$x_{\min} \leq x_t \leq x_{\max}. \tag{28}$$

In the thermal model of a building presented in Section 3, the symbols $\dot{Q}^{\mathrm{indoor}}_{\mathrm{z},t}$, $\dot{Q}^{\mathrm{heat}}_{\mathrm{z},t}$, and $\dot{Q}^{\mathrm{cool}}_{\mathrm{z},t}$ represent all internal thermal sources and are included in the matrix $\mathbf{U}$. However, in the optimization model for power system reliability, $\dot{Q}^{\mathrm{heat}}_{\mathrm{z},t}$ and $\dot{Q}^{\mathrm{cool}}_{\mathrm{z},t}$ are treated as optimization variables that contribute to the variable x_t as in Eq. (28). The indoor activities $\dot{Q}^{\mathrm{indoor}}_{\mathrm{z},t}$, however, are not optimized since they are still considered input parameters and, as such, are excluded from the optimization variable x_t.

The heating and cooling devices within the HVAC system cannot operate simultaneously. Therefore, the following constraint has to be added to the model:

$$\dot{Q}^{\mathrm{heat}}_{\mathrm{z},t} \dot{Q}^{\mathrm{cool}}_{\mathrm{z},t} = 0. \tag{29}$$

However, the current formulation of the optimization problem in Eqs. (19)–(29) is not directly applicable as a Mixed-Integer Linear Program (MILP) due to the non-linear nature of conditions (20) and (29). To overcome this, we can transform the problem into a set of linear constraints by introducing binary optimization variables $\alpha_{i,t}$ and β_t. The non-linear condition in Eq. (20) is linearized using the Big M method as follows:

$$-x_t \leq -P_i + P_t + M_1 \left(1 - \alpha_{i,t}\right), \tag{30}$$

$$x_t \leq P_i - P_t + M_2 \alpha_{i,t}, \tag{31}$$

where M_1 and M_2 are sufficiently large positive numbers. Similarly, the non-linear condition in Eq. (29) is linearized as follows:

$$\dot{Q}^{\mathrm{heat}}_{\mathrm{z},t} \leq M_3 \beta_t, \tag{32}$$

$$\dot{Q}^{\mathrm{cool}}_{\mathrm{z},t} \leq M_3 \left(1 - \beta_t\right), \tag{33}$$

where M_3 is another large positive number.

The resulting MILP optimization problem, defined by Eqs. (19)–(33), can now be solved to find the optimal set of variables Ω:

$$\Omega = \left\{ \alpha_{i,t}, \beta_t, x_t, T_{\mathrm{z},t}, T_{\mathrm{wo},t}, T_{\mathrm{wi},t}, Q^{\mathrm{heat}}_{\mathrm{z},t}, Q^{\mathrm{cool}}_{\mathrm{z},t} \right\}. \tag{34}$$

Among these, the most critical variables are $T_{\mathrm{z},t}$, $Q^{\mathrm{heat}}_{\mathrm{z},t}$, and $Q^{\mathrm{cool}}_{\mathrm{z},t}$. The variable $T_{\mathrm{z},t}$ represents the indoor temperature, which must remain within predefined limits to ensure occupant comfort. The terms $Q^{\mathrm{heat}}_{\mathrm{z},t}$ and $Q^{\mathrm{cool}}_{\mathrm{z},t}$ represent the electric energy required to maintain this temperature. The distribution of this energy over the observed period $\mathcal{T}$ directly impacts power system reliability, which is the primary focus of this research.

5. Case studies

The households modelled in these case studies are based on a standard residential building type with a single thermal zone. Each household is equipped with a centralized HVAC system capable of providing both heating and cooling, maintaining indoor temperatures within predefined comfort limits: 17 °C to 19 °C at night and 21 °C to 23 °C during the day. The thermal envelope of the buildings assumes moderate insulation, with parameters calibrated to represent typical construction in temperate climates. For simplicity, the buildings are considered unoccupied, eliminating internal heat gains from occupants or equipment. Solar radiation effects are also excluded to focus on the fundamental interactions between HVAC demand flexibility and power system reliability.

The impact of grid-interactive efficient buildings on the reliability of electric power systems is evaluated through two case studies (CSs):

- **CS1**: The households maintain the indoor temperature $T_{\mathrm{z},t}$ within specified limits using minimal heating and cooling power. The objective is formulated as:

$$J_{\mathrm{SC1}} = \underset{\Gamma}{\text{minimize}} \sum_{t \in \mathcal{T}} \left(\dot{Q}^{\mathrm{heat}}_{\mathrm{z},t} + \dot{Q}^{\mathrm{cool}}_{\mathrm{z},t} \right), \tag{35}$$

  subject to the constraints (21)–(26) and (29). In this scenario, the households do not provide demand flexibility to support the power system. Instead, they act as conventional consumers, drawing energy from the grid for their heating and cooling needs. Similar optimization model is presented in [21].

- **CS2**: The households contribute to maximizing power system reliability applying Eqs. (19)–(33) by leveraging grid-interactive efficient buildings, which enable demand flexibility. The indoor temperature $T_{\mathrm{z},t}$ is still maintained within predefined limits to prevent discomfort due to overheating or excessive cooling.

Table 1
Parameters of generators in power system.

Generator	Installed power (MW)	Availability
1	1273.0	0.9718
2	604.2	0.8954
3	319.2	0.8383
4	102.6	0.9923
5	129.2	0.9843
6	1065.9	0.9557
7	110.2	0.9886
8	85.5	0.9991

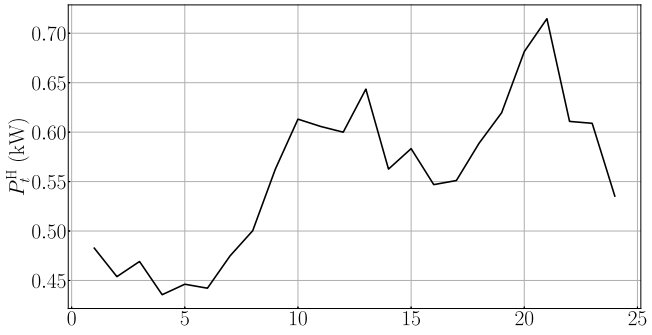

Fig. 6. Daily profile of the household consumption P_t^{H} without heating and cooling.

Table 2
Hourly consumption of electric energy.

Hour t	P_t^{PS} (MW)	$600.000\,P_t^{\mathrm{H}}$ (MW)	P_t (MW)
1	1033.07	289.63	1322.70
2	971.17	272.33	1243.50
3	928.28	281.52	1209.80
4	922.34	261.36	1183.70
5	907.17	267.73	1174.90
6	925.59	265.31	1190.90
7	966.68	284.92	1251.60
8	1089.52	300.18	1389.70
9	1199.26	337.54	1536.80
10	1285.62	367.88	1653.50
11	1286.84	363.46	1650.30
12	1297.02	359.98	1657.00
13	1344.40	386.10	1730.50
14	1253.83	337.57	1591.40
15	1181.42	349.98	1531.40
16	1168.75	328.15	1496.90
17	1206.26	330.64	1536.90
18	1214.19	353.21	1567.40
19	1367.61	371.79	1739.40
20	1364.25	408.85	1773.10
21	1434.27	428.83	1863.10
22	1359.09	366.51	1725.60
23	1203.74	365.36	1569.10
24	1112.42	321.18	1433.60

In both case studies, the power generation portfolio includes eight generators with installed capacities and availability factors as detailed in Table 1. These generators must meet the electricity demand specified in Table 2. The second column of Table 2 presents the power system demand, P_t^{PS}, excluding the residential electricity use of 600,000 households. Their electricity consumption, represented by $600{,}000\,P_t^{\mathrm{H}}$, is shown in the third column. This power is also supplied by the grid. For simplicity, all 600,000 households are considered identical, and the daily load profile of a single household (excluding heating and cooling) is illustrated in Fig. 6. The power required for heating and cooling is excluded from this diagram, as it is determined separately in each case study through the proposed optimization model. The final column in Table 2 shows the total hourly consumption P_t, which is used in the LOLE and EENS optimization as described in Section 2.

It is assumed that the households are unoccupied, thereby eliminating any indoor activities that would contribute to internal heat gains. Consequently, the term representing indoor heat gains, $Q_{\mathrm{z,t}}^{\mathrm{indoor}}$, is considered to be zero. Furthermore, the effects of solar radiation on the building envelope and windows are neglected, leading to $Q_{\mathrm{win,sol,t}}$ and $Q_{\mathrm{sol,t}}$ being set to zero as well. These assumptions are considered reasonable and do not compromise the validity of the research conclusions. Specifically, the excluded parameters, internal heat gains and solar radiation, are input variables within the model. While they are set to zero in this analysis, the model can accommodate non-zero values for these parameters if needed. The focus of this study is on the fundamental interactions within the system under controlled conditions, and the exclusion of these variables allows for a more straightforward analysis of the primary effects under study. Moreover, these assumptions help to isolate the impact of other factors, ensuring that the results are not confounded by the variability introduced by internal heat gains or solar radiation.

Figs. 7 and 8 show the ambient temperature $T_{\mathrm{o},t}$ and the resulting optimal indoor temperature $T_{\mathrm{z},t}$ in CS1 and CS2, respectively. The observed period spans two days, July 22 and 23, 2024, with a simulation time step of one minute. Both days feature identical ambient temperatures $T_{\mathrm{o},t}$ to highlight the transient effects at the beginning of the simulation, which diminish within a few minutes. These transients are influenced by the initial values of the optimization variables $T_{\mathrm{wo},0}$, $T_{\mathrm{wi},0}$, $T_{\mathrm{z},0}$ and inputs $T_{\mathrm{o},0}$, $\dot{Q}_{\mathrm{z},0}^{\mathrm{indoor}}$, $\dot{Q}_{\mathrm{z},0}^{\mathrm{heat}}$, $\dot{Q}_{\mathrm{z},0}^{\mathrm{cool}}$, $\dot{Q}_{\mathrm{win,sol},0}$, $\dot{Q}_{\mathrm{sol},0}$, which comprise matrices $\mathbf{T}_0$ and $\mathbf{U}_0$.

The results indicate that in both case studies, the indoor temperature $T_{\mathrm{z},t}$ remains within the prescribed bounds, $T_{\mathrm{z},t}^{\mathrm{min}}$ and $T_{\mathrm{z},t}^{\mathrm{max}}$, ensuring that comfort levels are maintained throughout the observed period $\mathcal{T}$. In CS1, during periods of low ambient temperature $T_{\mathrm{o},t}$, the indoor temperature $T_{\mathrm{z},t}$ tends to reach the lower allowable limit, thereby minimizing the required heating energy. Conversely, during periods of high ambient temperature $T_{\mathrm{o},t}$, $T_{\mathrm{z},t}$ approaches the upper allowable limit, reducing the need for cooling energy. This behaviour reflects the building's thermal dynamics, with $T_{\mathrm{z},t}$ oscillating close to the upper bound in CS1.

In contrast, CS2 shows a more dynamic temperature profile, with noticeable fluctuations, including peaks and troughs. These variations suggest that heating and cooling periods were intentionally shifted or delayed to provide demand-side flexibility, particularly during peak demand hours. As a result, $T_{\mathrm{z},t}$ in CS2 is generally closer to the lower bound, $T_{\mathrm{z},t}^{\mathrm{min}}$, during these high-demand periods. This approach enhances the reliability of the power supply system by actively managing demand response, allowing the system to be more resilient. The more adaptive temperature controls in CS2 align with power system needs, reducing the overall strain on the grid during high-demand periods.

Figs. 9 and 10 illustrate the electric power required for heating and cooling during the observed period $\mathcal{T}$, denoted as $\dot{Q}_{\mathrm{z},t}^{\mathrm{heat}}$ and $\dot{Q}_{\mathrm{z},t}^{\mathrm{cool}}$, for a single household in scenarios SC1 and SC2, respectively. For simplicity in this analysis, both the heating and cooling coefficients of performance (COP_{heat} and COP_{cool}) are set to 1. The total energy consumption in SC1 and SC2 is 3.42 kWh and 5.18 kWh, respectively. This difference is expected, as the objective in SC1 is to minimize the energy required for heating and cooling.

Fig. 11 presents the total hourly electricity consumption, P_t, which is also summarized in Table 2. This figure includes the residential consumption of 600,000 households, excluding heating and cooling, as well as the consumption of other network users. The reference consumption, P_t, is used for both simulated scenarios, with the additional consumption required for heating and cooling 600,000 households added as x_t^{SC1} and x_t^{SC2}. The total electricity consumption during the observed period $\mathcal{T}$ for SC1 and SC2 is 74,096.74MWh and 75,150.96MWh, respectively.

For both case studies, the LOLE is calculated as a measure of power system reliability. The LOLE values obtained are 0.082 h and

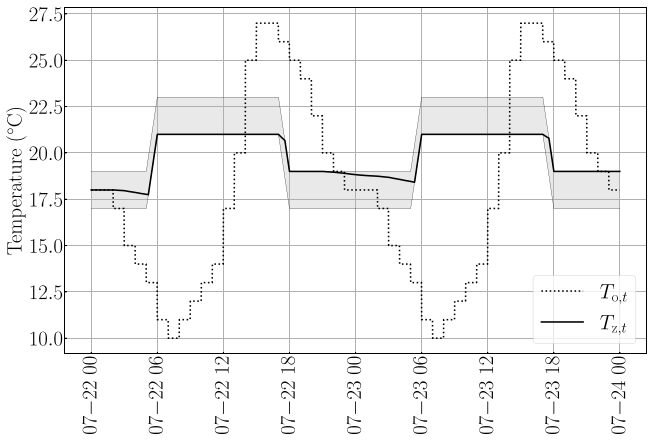

Fig. 7. Ambient temperature $T_{o,t}$ and optimal indoor temperature $T_{z,t}$ within the limits in CS1.

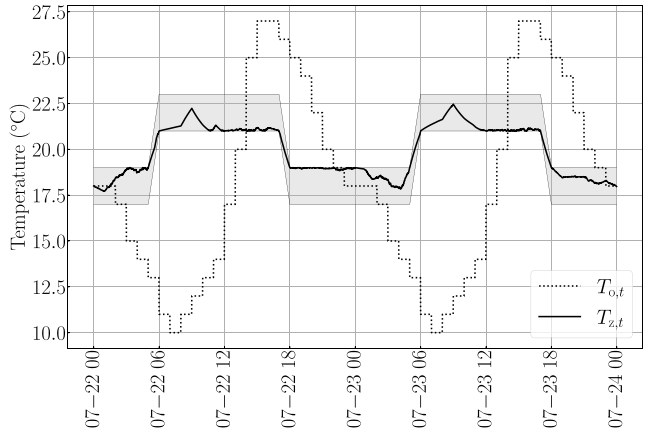

Fig. 8. Ambient temperature $T_{o,t}$ and optimal indoor temperature $T_{z,t}$ within the limits in CS2.

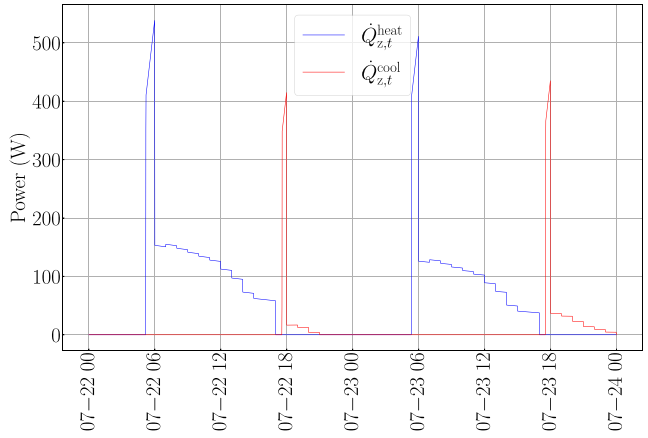

Fig. 9. Electric power required for heating and cooling of one household in CS1.

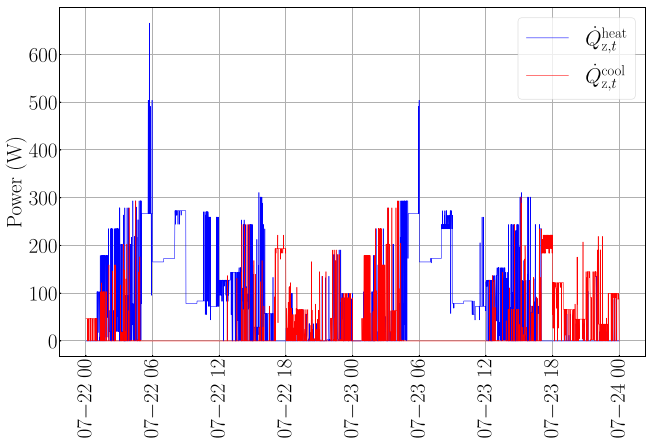

Fig. 10. Electric power required for heating and cooling of one household in CS2.

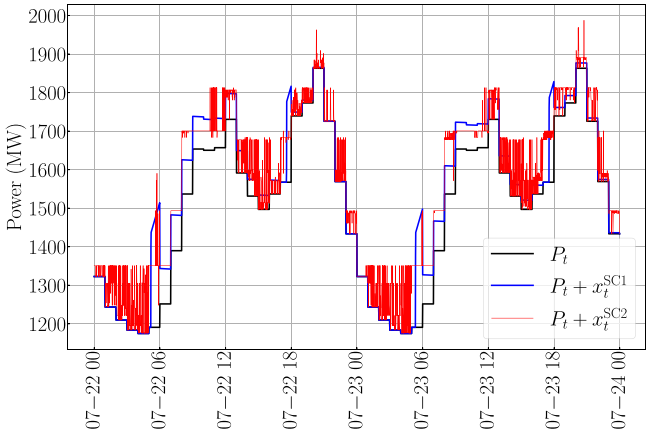

Fig. 11. Total electricity consumption in CS1 and CS2.

0.075 h for the observed period $\mathcal{T}$ of two days. Extrapolated on a yearly basis, the expected LOLE values would be 14.81 h and 13.65 h. In this study, LOLE improves by 7.82% when 600,000 households with grid-interactive efficient buildings are included in the reliability optimization, despite the increased total electricity consumption in SC2.

Considering EENS as another measure of power system reliability, the values obtained for SC1 and SC2 are 135.39MWh and 125.88MWh for the observed period $\mathcal{T}$ of two days, respectively, corresponding to 24,708.76MWh and 22,972.99MWh annually. By applying the proposed optimization model, EENS improves by 7.02% with the engagement of 600,000 households.

It is important to note that the case studies were conducted under uniform climatic conditions and building types to ensure consistency and simplify the analysis. However, variations in climate, such as hotter or colder regions, or differences in building characteristics, such as higher or lower thermal inertia or insulation levels, could significantly impact the results. For instance, buildings in colder climates may have higher heating demands, while those in warmer climates may rely more on cooling, influencing the flexibility potential. Similarly, well-insulated buildings with higher thermal inertia may offer greater demand flexibility compared to poorly insulated ones. These factors should be explored in future research to validate the applicability of the proposed model to diverse real-world scenarios.

5.1. Complementary grid technologies

While the demand flexibility provided by GEBs significantly contributes to grid reliability, other grid-supporting technologies, such as battery storage and flexible line ratings, further enhance system resilience. Battery storage systems provide essential backup power during peak loads or outages, complementing GEB demand response. Similarly, dynamic line ratings allow for adjustments in the transmission system's capacity based on real-time conditions, which can help reduce stress on the grid during critical periods.

Studies have shown the benefits of integrating GEBs with additional grid technologies to achieve a comprehensive approach to grid reliability. For example, [22] highlights how flexible line ratings can improve resilience during high-demand periods. Additionally, [23,24] demonstrate the combined benefits of distributed generation, dynamic line ratings, and storage technologies in supporting grid stability.

Integrating GEBs with these grid-supporting technologies offers a holistic pathway to enhanced power system reliability. By combining demand flexibility with advanced storage and transmission capabilities, the grid can better manage diverse operating conditions. This approach provides opportunities for future research and implementation, where GEBs and advanced grid technologies collaborate to address the complexities of modern power systems.

5.2. Potential impacts on other reliability metrics

While this study focused on LOLE and EENS as key reliability metrics, power system reliability is inherently multidimensional and includes additional aspects such as frequency regulation and voltage stability. GEBs, with their ability to dynamically adjust demand in response to grid conditions, hold significant potential to impact these metrics. For instance, by modulating demand in real-time, GEBs can help stabilize frequency fluctuations during periods of rapid load changes or generation imbalances. Similarly, their flexible operation can improve voltage profiles by reducing stress on local distribution networks during peak load conditions.

These additional dimensions of reliability were not included in the current study due to the specific focus on resource adequacy metrics (LOLE and EENS) and the complexity of modelling real-time grid dynamics within the scope of this research. However, future work will investigate how GEBs can contribute to these areas, complementing their role in improving resource adequacy and enhancing overall grid stability.

5.3. Scalability and application to complex systems

While this study focuses on a single-zone thermal model for simplicity and computational feasibility, the proposed optimization framework is designed to be scalable and applicable to more complex real-world scenarios. Extending the model to multi-zone buildings or systems involving many buildings with varying thermal characteristics would require enhancements to account for the heterogeneity of these systems.

For multi-zone applications, the model could integrate individual zone dynamics, capturing variations in internal heat gains, solar radiation, and occupancy patterns across different zones within a building. This would allow the optimization framework to manage interactions between zones, such as heat transfer through shared walls, while maintaining indoor comfort in each zone. The Ref. [25] demonstrates a model-based optimal control strategy for Variable Air Volume air-conditioning systems in multi-zone buildings, using genetic algorithms to enhance control efficiency and scalability. Similarly, [26] provides an overview of HVAC system simulations in multi-zone buildings, discussing the scalability challenges and strategies to address computational complexity in such models.

For systems involving multiple buildings, the optimization would need to account for diverse building types, thermal properties, and demand flexibility profiles. This could be achieved by clustering buildings with similar characteristics and incorporating these clusters into the optimization model. Aggregating demand flexibility across clusters could simplify the computation while preserving the benefits of GEB integration at the system level. The article [27] reviews methods for predicting building energy consumption in multi-zone systems and highlight techniques for ensuring scalability in complex scenarios. The paper [28] discusses state-of-the-art modelling methods that emphasize the need for multi-building energy performance predictions, providing insights into how such approaches can be integrated into system-level optimization frameworks.

Scalability also poses challenges, particularly in terms of computational complexity and data requirements. Incorporating additional zones or buildings would increase the number of variables and constraints, potentially requiring advanced computational techniques, such as parallel processing or heuristic algorithms, to solve the optimization problem efficiently. Additionally, accurate data on thermal properties and flexibility potentials for diverse buildings would be necessary to ensure realistic modelling outcomes. Future research will explore these extensions to validate the scalability of the model and its applicability to large-scale systems, including multi-zone and multi-building scenarios.

5.4. Sensitivity analysis: Comfort limits and thermal inertia

The flexibility potential of GEBs is significantly influenced by the indoor comfort limits and the thermal inertia of the building. Comfort limits define the allowable temperature range within which HVAC systems can operate without compromising occupant comfort. Narrower comfort ranges constrain demand flexibility, as the system has less room to adjust HVAC operations without violating comfort constraints. Conversely, wider ranges provide greater flexibility, enabling more significant load shifting and potentially improving grid reliability metrics such as LOLE and EENS.

Thermal inertia, representing the building's capacity to retain heat, also plays a critical role. Buildings with high thermal inertia can maintain indoor temperatures within comfort limits for longer periods without active heating or cooling, offering greater flexibility. In contrast, buildings with low thermal inertia require more frequent HVAC adjustments, which limits their ability to contribute to demand-side flexibility. These theoretical insights suggest that the choice of comfort limits and thermal properties is crucial when scaling GEB models to diverse building types.

While no additional simulations were conducted in this study, these conclusions align with existing knowledge and highlight key factors that should be considered in future research and model extensions.

6. Conclusion

This paper introduces a novel method for the direct optimization of power system reliability, leveraging the potential of GEBs. The proposed solution involves thermal modelling of buildings to simulate indoor temperature dynamics, considering the building envelope characteristics and internal thermal mass. The research findings demonstrate that households can effectively enhance power system reliability by utilizing the available demand flexibility of their buildings. Future research will focus on an economic assessment of this support, comparing it with existing services provided by conventional power plants and demand-side flexibility. Additionally, the influence of indoor activities on GEB demand flexibility and its contribution to power system reliability will be explored in greater detail, employing more advanced thermal modelling techniques. Future research will also focus on validating the thermal model with real-world data from grid-interactive efficient buildings. This step will enhance the accuracy and practical relevance of the findings, ensuring that the proposed model is robust and applicable under diverse operational conditions.

CRediT authorship contribution statement

Miloš Pantoš: Writing – original draft, Software, Methodology, Conceptualization. **Lucija Lukas:** Writing – original draft, Methodology, Conceptualization.

Declaration of competing interest

The authors declare that they have no known competing financial interests or personal relationships that could have appeared to influence the work reported in this paper.

Data availability

No data was used for the research described in the article.

References

[1] Chen R, Xu P, Chen L, Yao H. Did electrification of the building sector achieve carbon mitigation? A provincial retrospection in China. Build Environ 2024;248:111084. http://dx.doi.org/10.1016/j.buildenv.2023.111084, URL https://www.sciencedirect.com/science/article/pii/S0360132323011113.

[2] Wei C, Wu Q, Xu J, Sun Y, Jin X, Liao S, et al. Distributed scheduling of smart buildings to smooth power fluctuations considering load rebound. Appl Energy 2020;276:115396. http://dx.doi.org/10.1016/j.apenergy.2020.115396, URL https://www.sciencedirect.com/science/article/pii/S0306261920309089.

[3] Chu W, Zhang Y, He W, Zhang S, Hu Z, Ru B, et al. Research on flexible allocation strategy of power grid interactive buildings based on multiple optimization objectives. Energy 2023;278:127943. http://dx.doi.org/10.1016/j.energy.2023.127943, URL https://www.sciencedirect.com/science/article/pii/S0360544223013373.

[4] Yue L, Niu J, Tian Z, Lin Q, Lu Y. A three-dimensional evaluation method for building energy systems to guide power grid-friendly interactions during the planning and operational stages. J Build Eng 2024;86:108816. http://dx.doi.org/10.1016/j.jobe.2024.108816, URL https://www.sciencedirect.com/science/article/pii/S235271022400384X.

[5] Neukomm M, Nubbe V, Fares R. Grid-interactive efficient buildings technical report series: Overview of research challenges and gaps, http://dx.doi.org/10.2172/1577966, URL https://www.osti.gov/biblio/1577966.

[6] Satchwell A, Piette M, Khandekar A, Granderson J, Frick N, Hledik R, et al. A national roadmap for grid-interactive efficient buildings. Tech. rep., Lawrence Berkeley National Laboratory; 2021, URL https://escholarship.org/uc/item/78k303s5.

[7] Abdou N, El Mghouchi Y, Hamdaoui S, Mhamed M. Optimal building envelope design and renewable energy systems size for net-zero energy building in Tetouan (Morocco). In: 2021 9th international renewable and sustainable energy conference. 2021, p. 1–6. http://dx.doi.org/10.1109/IRSEC53969.2021.9741188.

[8] Khatibi M, Rahnama S, Vogler-Finck P, Dimon Bendtsen J, Afshari A. Towards designing an aggregator to activate the energy flexibility of multi-zone buildings using a hierarchical model-based scheme. Appl Energy 2023;333:120562. http://dx.doi.org/10.1016/j.apenergy.2022.120562, URL https://www.sciencedirect.com/science/article/pii/S0306261922018190.

[9] Fontenot H, Ayyagari KS, Dong B, Gatsis N, Taha A. Buildings-to-distribution-network integration for coordinated voltage regulation and building energy management via distributed resource flexibility. Sustainable Cities Soc 2021;69:102832. http://dx.doi.org/10.1016/j.scs.2021.102832, URL https://www.sciencedirect.com/science/article/pii/S2210670721001220.

[10] Utama C, Troitzsch S, Thakur J. Demand-side flexibility and demand-side bidding for flexible loads in air-conditioned buildings. Appl Energy 2021;285:116418. http://dx.doi.org/10.1016/j.apenergy.2020.116418, URL https://www.sciencedirect.com/science/article/pii/S0306261920317815.

[11] Wang Y, Xu Y, Tang Y. Distributed aggregation control of grid-interactive smart buildings for power system frequency support. Appl Energy 2019;251:113371. http://dx.doi.org/10.1016/j.apenergy.2019.113371, URL https://www.sciencedirect.com/science/article/pii/S0306261919310451.

[12] Peiqiang L, Chengyu Z, Zuoyun T, Piao X, Xuqiong Y. Integrated energy collaborative optimal dispatch considering energy flexible building in smart grid. In: 2019 IEEE innovative smart grid technologies - Asia. 2019, p. 3799–803. http://dx.doi.org/10.1109/ISGT-Asia.2019.8881586.

[13] Hanif S, Gruentgens C, Massier T, Hamacher T, Reindl T. Cost-optimal operation for a flexible building with local PV in a Singaporean environment. In: 2016 IEEE power & energy society innovative smart grid technologies conference. 2016, p. 1–5. http://dx.doi.org/10.1109/ISGT.2016.7781232.

[14] Ye Y, Faulkner CA, Xu R, Huang S, Liu Y, Vrabie DL, et al. System modeling for grid-interactive efficient building applications. J Build Eng 2023;69:106148. http://dx.doi.org/10.1016/j.jobe.2023.106148, URL https://www.sciencedirect.com/science/article/pii/S2352710223003273.

[15] Klanatsky P, Veynandt F, Heschl C. Grey-box model for model predictive control of buildings. Energy Build 2023;300:113624. http://dx.doi.org/10.1016/j.enbuild.2023.113624, URL https://www.sciencedirect.com/science/article/pii/S037877882300854X.

[16] Wang S, Xu X. Parameter estimation of internal thermal mass of building dynamic models using genetic algorithm. Energy Convers Manage 2006;47(13):1927–41. http://dx.doi.org/10.1016/j.enconman.2005.09.011, URL https://www.sciencedirect.com/science/article/pii/S0196890405002311.

[17] Li Y, O'Neill Z, Zhang L, Chen J, Im P, DeGraw J. Grey-box modeling and application for building energy simulations - A critical review. Renew Sustain Energy Rev 2021;146:111174. http://dx.doi.org/10.1016/j.rser.2021.111174, URL https://www.sciencedirect.com/science/article/pii/S1364032121004639.

[18] Božič D, Pantoš M. Impact of electric-drive vehicles on power system reliability. Energy 2015;83:511–20. http://dx.doi.org/10.1016/j.energy.2015.02.055, URL https://www.sciencedirect.com/science/article/pii/S0360544215002108.

[19] Shi J, Teh J, Alharbi B, Lai C-M. Load forecasting for regional integrated energy system based on two-phase decomposition and mixture prediction model. Energy 2024;297:131236. http://dx.doi.org/10.1016/j.energy.2024.131236, URL https://www.sciencedirect.com/science/article/pii/S0360544224010090.

[20] Shi J, Teh J. Load forecasting for regional integrated energy system based on complementary ensemble empirical mode decomposition and multi-model fusion. Appl Energy 2024;353:122146. http://dx.doi.org/10.1016/j.apenergy.2023.122146, URL https://www.sciencedirect.com/science/article/pii/S0306261923015106.

[21] Mai W, Chung CY. Model predictive control based on thermal dynamic building model in the demand-side management. In: 2016 IEEE power and energy society general meeting. 2016, p. 1–5. http://dx.doi.org/10.1109/PESGM.2016.7741437.

[22] Lai C-M, Teh J, Alharbi B, AlKassem A, Aljabr A, Alshammari N. Optimisation of generation unit commitment and network topology with the dynamic thermal rating system considering N-1 reliability. Electr Power Syst Res 2023;221:109444. http://dx.doi.org/10.1016/j.epsr.2023.109444, URL https://www.sciencedirect.com/science/article/pii/S0378779623003334.

[23] Yang L, Teh J, Alharbi B. Optimizing distributed generation and energy storage in distribution networks: Harnessing metaheuristic algorithms with dynamic thermal rating technology. J Energy Storage 2024;91:111989. http://dx.doi.org/10.1016/j.est.2024.111989, URL https://www.sciencedirect.com/science/article/pii/S2352152X24015755.

[24] Song T, Teh J. Coordinated integration of wind energy in microgrids: A dual strategy approach leveraging dynamic thermal line rating and electric vehicle scheduling. Sustain Energy Grids Netw 2024;38:101299. http://dx.doi.org/10.1016/j.segan.2024.101299, URL https://www.sciencedirect.com/science/article/pii/S2352467724000286.

[25] Wang S, Jin X. Model-based optimal control of VAV air-conditioning system using genetic algorithm. Build Environ 2000;35(6):471–87. http://dx.doi.org/10.1016/S0360-1323(99)00032-3, URL https://www.sciencedirect.com/science/article/pii/S0360132399000323.

[26] Trčka M, Hensen JL. Overview of HVAC system simulation. Autom Constr 2010;19(2):93–9. http://dx.doi.org/10.1016/j.autcon.2009.11.019, URL https://www.sciencedirect.com/science/article/pii/S0926580509001897.

[27] xiang Zhao H, Magoulès F. A review on the prediction of building energy consumption. Renew Sustain Energy Rev 2012;16(6):3586–92. http://dx.doi.org/10.1016/j.rser.2012.02.049, URL https://www.sciencedirect.com/science/article/pii/S1364032112001438.

[28] Foucquier A, Robert S, Suard F, Stéphan L, Jay A. State of the art in building modelling and energy performances prediction: A review. Renew Sustain Energy Rev 2013;23:272–88. http://dx.doi.org/10.1016/j.rser.2013.03.004, URL https://www.sciencedirect.com/science/article/pii/S1364032113001536.